Received: 3 February 2022 | Revised: 27 September 2022 | Accepted: 3 November 2022

DOI: 10.1002/rra.4083

SPECIAL ISSUE PAPER

WILEY

Evaluating the risk of fish stranding due to hydropeaking in a large continental river

Sarah E. Glowa[1,2] | Douglas A. Watkinson[1] | Timothy D. Jardine[2] | Eva C. Enders[3]

[1]Fisheries and Oceans Canada, Freshwater Institute, Winnipeg, Canada

[2]School of Environment and Sustainability, University of Saskatchewan, Saskatoon, Canada

[3]Institut National de la Recherche Scientifique, Eau Terre Environnement Research Centre, Québec, Canada

Correspondence
Sarah E. Glowa, Fisheries and Oceans Canada, Freshwater Institute, Winnipeg, Manitoba, Canada.
Email: sarah.glowa@dfo-mpo.gc.ca

Funding information
Fisheries and Oceans Canada

Abstract

With the continuous development of hydropower on a global scale, stranding of freshwater fishes is of growing concern, and an understanding of the mechanisms and variables affecting fish stranding in hydropeaking rivers is urgently needed. In particular, a methodology is required to identify the magnitude and timing at which fish stranding occurs in relation to environmental conditions. Here, we studied fish stranding in three reaches downstream of a hydropeaking generation station in the Saskatchewan River, Saskatchewan, Canada, using an innovative remote photography approach with 45 trail cameras and traditional transect monitoring, conducting 323 transects. We observed that juvenile sport and commercial fish species are stranding at a higher proportion than small bodied fish species. The remote photography approach provided more precise fish stranding timing and associated the environmental and physical conditions with a given stranding event, but captured fewer fish and only rarely allowed species identification. The comparison of the two methodologies resulted in similar stranded fish densities, but the remote photography allowed for continuous observations whereas the transect monitoring was limited by the observer availability in the field. Remote photography allowed for additional information on the scavenging of stranded fish, with scavenging occurring on average within 240 minutes of the fish being stranded. The probability of fish stranding increased significantly with increasing water temperature and substrate particle size resulted in greater stranding on finer substrates. Our findings have important implications for hydroelectric flow management by introducing an innovative, standardized method to study the effects of hydropeaking events on fish stranding that can be applied to increase our understanding of the impacts of hydropeaking on fish communities.

KEYWORDS
hydroelectric station, remote photography, Saskatchewan River, transect monitoring

1 | INTRODUCTION

Climate change and increasing energy demands are driving the need for renewable energy. Hydropower is one of the renewable resource options that continues to grow globally (Zarfl, Lumsdon, Berlekamp, Tydecks, & Tockner, 2015). Albeit having the advantages of a renewable resource, the development and operation of hydroelectric generating stations can have negative impacts on natural ecosystem processes (e.g., hydrology, sediment transport; Bruder et al., 2016; Rosenberg, McCully, & Pringle, 2000), and affect fish

survival and fish community composition and structure (Algera et al., 2020; Enders et al., 2019; Guisández, Pérez-Díaz, & Wilhelmi, 2013; Silva et al., 2018; Smokorowski, 2022; Winemiller et al., 2016).

Anthropogenic flow fluctuations, defined as hydropeaking, occur when storage dams are operated to meet diurnal changes in electricity demand by modifying sub-daily changes in flow (Smokorowski, 2022). One of the direct impacts from hydropeaking is fish stranding (Nagrodski, Raby, Hasler, Taylor, & Cooke, 2012). Fish stranding occurs when water levels decrease and fish become trapped on the river edge or in pools that become disconnected from the thalweg, resulting in increased risk of desiccation, asphyxiation, freezing, and predation by avian and mammalian predators (Larrieu, Pasternack, & Schwindt, 2021; Nagrodski et al., 2012). Fish communities that are subject to hydropeaking are threatened with a noticeable decrease in overall fish abundance (Moog, 1994) and can have fewer small-bodied and juvenile fish (Enders, Watkinson, Ghamry, Mills, & Franzin, 2017). Stranding is influenced by physical factors including hydropeaking regime, water temperature, substrate particle size, slope, and wetted history (Nagrodski et al., 2012; Smokorowski, 2022), but understanding the interactions and cumulative effects of these variables in determining stranding risk is still limited. Previous fish stranding studies have focused on only a few species, notably salmonids (Nagrodski et al., 2012), whereas fish communities in large continental rivers are less well studied.

Different methods have been used to assess fish stranding, which include counting fish in natural settings such as transect monitoring (Irvine, Thorley, Westcott, Schmidt, & Derosa, 2015; Moore & Gregory, 2011) or in modified settings such as enclosures and isolated channels (Auer, Zeiringer, Führer, Tonolla, & Schmutz, 2017; Bradford, 1997; Flodmark et al., 2002; Irvine, Oussoren, Baxter, & Schmidt, 2009; Puffer et al., 2015; Saltveit, Halleraker, Arnekleiv, & Harby, 2001), and within a laboratory setting (Fisk, Kwak, Heise, & Sessions, 2013). In general, stranding is directly linked to the recession of water. Subsequently, if stranding assessments are not conducted at the time of the water recession, stranding events can be missed. Therefore, there is a need for a standardized method that, on the one hand, does not modify the riverine ecosystem and, on the other hand, is able to capture stranding events as they happen independent of potential limited observer availability (Nagrodski et al., 2012). Solutions can be found in remote photography, which is commonly used in applications where it may be difficult to observe or capture a phenomenon when it transpires, as it eliminates the need for on-site surveys and allows for continuous monitoring over prolonged periods of time (Cutler & Swann, 1999). Trail cameras have previously been used to monitor changes in water level, including when channels become dewatered (Eppehimer, Enger, Ebenal, Rocha, & Bogan, 2021; Larrieu & Pasternack, 2021). Here, we extended that approach by depicting the potential for stranding through water level changes as well as by quantifying the fish stranding densities in the camera image.

Fish stranding has been identified as an issue in the Saskatchewan River, Saskatchewan, Canada, due to the hydropeaking operation of the E.B. Campbell Hydroelectric Station. This station has been operating on a hydropeaking regime since its commission in 1963 (Watkinson, Ghamry, & Enders, 2020). In 2004, Fisheries and Oceans Canada's Fish and Fish Habitat Protection Program enforced a minimum flow requirement of 75 $m^3 \cdot s^{-1}$ (Enders et al., 2017). Currently, the hydropeaking continues with daily discharge releases from the powerhouse ranging as large as ~100 to 1,000 $m^3 \cdot s^{-1}$, leading to regular fish stranding events (Green, Jardine, Weber, & Janz, 2020).

The objectives of this study were to (1) quantify stranding events that are occurring due to hydropeaking downstream of E.B. Campbell Hydroelectric Station; (2) identify species and estimate the size of fish being stranded in comparison to local species composition; (3) compare time lapse cameras to conventional transect monitoring to estimate fish stranding; and (4) assess what variables (i.e., horizontal and vertical ramping rate, water temperature, substrate, wetted history) influence fish stranding.

2 | METHODS

2.1 | Study site

The E.B. Campbell Hydroelectric Station was constructed in 1962 on the Saskatchewan River in East-Central Saskatchewan and has a generation capacity of 289 MW (Watkinson et al., 2020) (Figure 1). The natural hydrograph of the Saskatchewan River follows a pattern of two annual flood peaks, representing the surrounding snow and ice melt in May, followed by the snowpack melt from the Rocky Mountains, Alberta, in July (Enders et al., 2017). The E.B. Campbell Hydroelectric Station is typically operated with a hydropeaking regime to address daily peak energy demands.

The study site was located downstream of the E.B. Campbell Hydroelectric Station and had a total length of 16 km. It was further divided into three study reaches (Figure 1). The reaches varied in substrate, slope, and ramping rate, allowing for observations of fish stranding over a variety of different habitats. Reach 1 (N 53.69022 W 103.34913) is ~1 km long and is situated in the original, pre-1962 river channel that is now bypassed by the E.B. Campbell Hydroelectric Station. Reach 1 is typically back watered daily due to the hydropeaking operation. Reach 2 is situated ~9 km downstream from the hydroelectric station and is ~1 km long (N 53.71792 W 103.23237). Reach 3 is located ~13 km downstream from the hydroelectric station and is ~1.2 km long (N 53.72514 W 103.17578). Two boat launches in the local area were used for additional sites to conduct transect monitoring that represent fish stranding outside of the three reaches (Figure 1).

2.2 | Remote photography

In order to estimate fish stranding remotely, time lapse cameras (Boly trail camera, model 2G2060-D, Victoriaville, QC, Canada) were used to take pictures of the riverbed. The cameras were secured to a

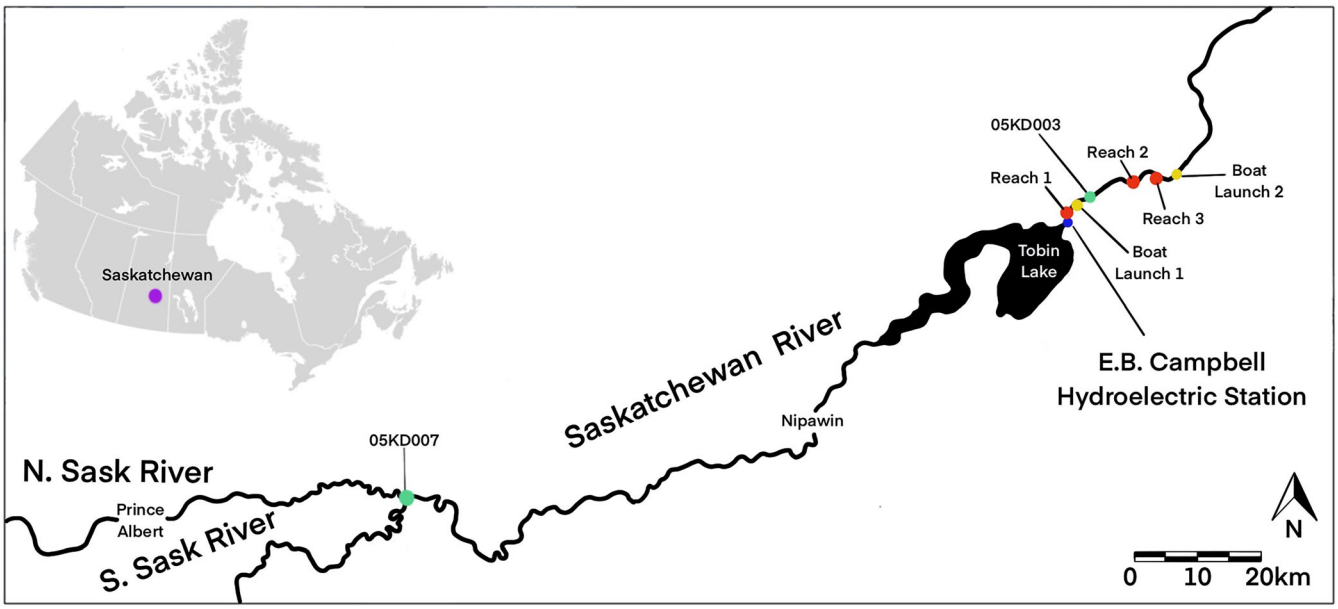

FIGURE 1 Map of the study site in Saskatchewan River, Saskatchewan, Canada. Study reaches are indicated in red, boat launches in yellow, and the Water Survey of Canada's gauging stations in green. [Color figure can be viewed at wileyonlinelibrary.com]

custom-made camera mount (Figure 2) pointed downward, perpendicular to the slope of the riverbed. Each mount consisted of three 0.635 mm double braided nylon ropes, 30 × 30 cm concrete paving stone, 30 cm steel fence post stakes, a 2.5 cm square aluminum tube, a 0.79 cm pin with keeper, 1.9 cm square aluminum tube, 5 × 15 cm dimensional lumber, a 1.27 cm eye bolt, and the trail camera housing (Figure 2). Camera mounts were on average 367.7 cm high (minimum 350.5 cm, maximum 378.5 cm, standard deviation 5.8 cm, camera lens relative to substrate) above the riverbed, resulting in a surface area ranging from 6.50 to 7.26 m^2 that was examined for stranded fish.

Cameras were placed in locations that were identified as having the potential for fish stranding, which was determined using photogrammetry and bathymetry mapping conducted in 2019. Photogrammetry mapping was performed during low discharges (averaging 375.1 $m^3 \cdot s^{-1}$) that exposed the available riverbed, while bathymetry was conducted during high discharges (averaging 751.1 $m^3 \cdot s^{-1}$). The photogrammetry map and bathymetry map were then imported into ArcGIS Pro (Redlands, CA, USA) to develop a map outlining low and high-water levels. Locations of overlap were considered areas of stranding potential. At each of the three reaches within the alternating wet/dry zone, 15 locations were randomly selected for the camera installation by overlaying site maps with a 50 m-by-50 m grid in RStudio (RStudio Team, 2020), using the exactextractr (v0.7.2; Baston, 2021), rgeos (v0.5-8; Bivand & Rundel, 2021), and rgdal (v1.5-27; Bivand, Keitt, & Rowlingson, 2021) packages. Camera mounts were placed in the centre coordinates of the randomly selected quadrats. Images were taken at 30 minutes intervals to capture receding water levels and stranded fish.

The cameras were placed as soon after ice-out as possible and remaining in place as late in the ice-free season as possible. In Reach 1, they were set up May 14–16, 2021, and due to COVID-19 restrictions, the cameras in Reaches 2 and 3 were only set up a month later, June 14–19, 2021. Cameras stayed on site continually capturing images until October 13–15, 2021. Once a month, the cameras were visited to download the images and ensure the mount was stable.

2.3 | Transect monitoring

To search for stranded fish by direct observation, transect monitoring was conducted monthly during the same site visits when cameras were installed, maintained, and images downloaded. In total, six sampling periods occurred at Reach 1 and five sampling periods at Reaches 2 and 3. Within each reach, 15 transects located between camera mounts were surveyed. Three additional transects were conducted in Reaches 1 and 2 and two in Reach 3 to extend surveys along the shorelines (Figure 3). In addition, transect monitoring was performed at each of the boat launches that are accessible by road (N 53.692633 W 103.326204 and N 53.729585 W 103.123385, respectively). Sampling was conducted in the early morning during lower water levels. All transects were surveyed ~1.5 m on either side of the surveyor line and ranged in length from 44 to 420 m, so stranding was calculated on a per area basis. All fish in the transects were fixed in formalin and brought to the laboratory for identification, measured (fork and total length), and weighed. We assumed that stranded fish found during transect monitoring stranded at the previous wet-dry cycle, despite the possibility that the fish might have stayed in place since multiple hydropeaking cycles.

In order to determine stranding rates in the absence of hydropeaking, transect monitoring was conducted monthly at two reference sites on the South Saskatchewan River in Saskatoon, Saskatchewan, upstream from the E.B. Campbell Hydroelectric Station. This reach

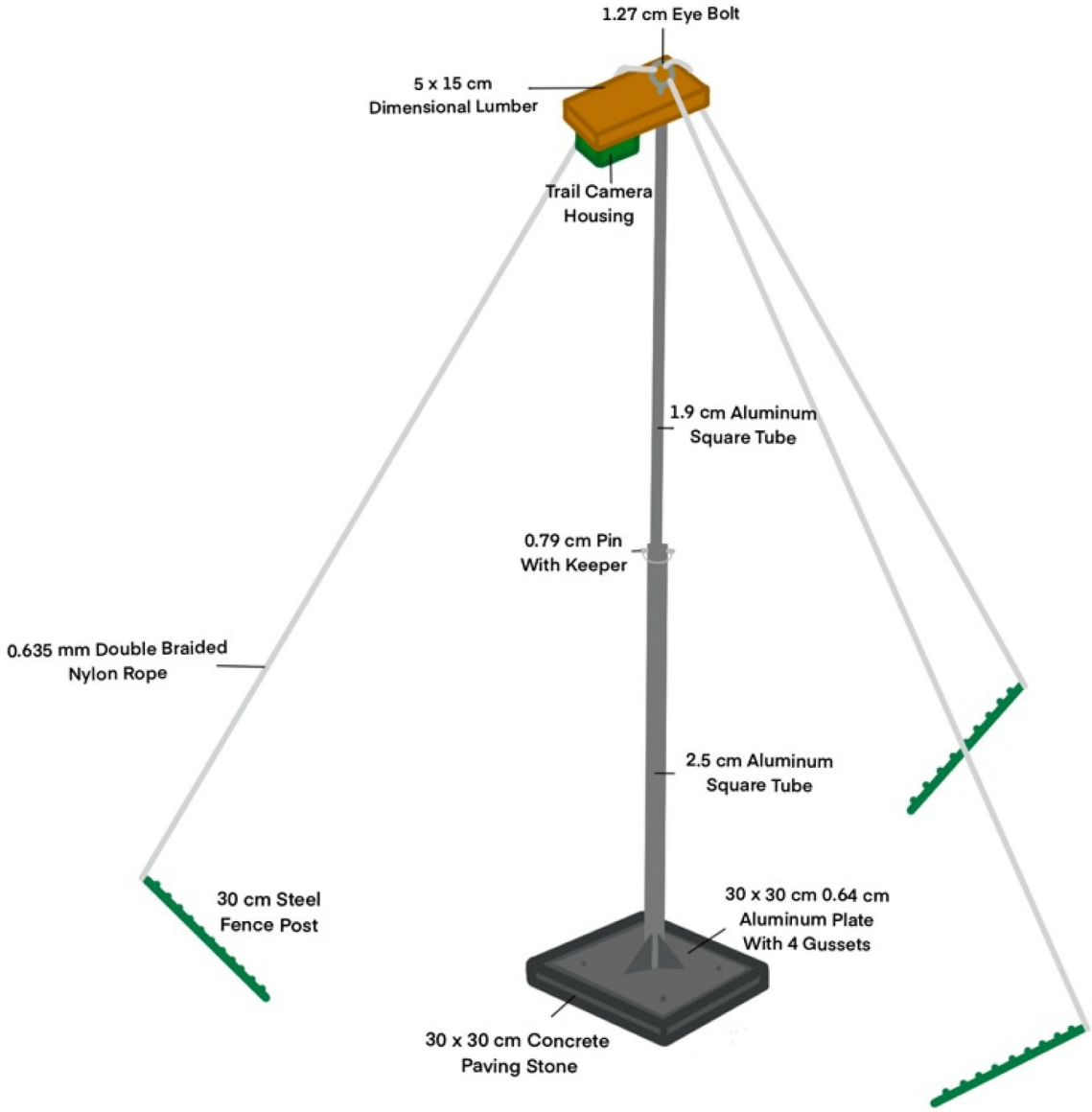

FIGURE 2 Schematic of the camera setup for the downward-facing time lapse cameras. The landscape block and fence post stakes are recessed into the natural riverbed substrate. [Color figure can be viewed at wileyonlinelibrary.com]

experiences only subtle daily changes (<5 cm per day) in water level due to attenuation of hydropeaking flows from the Coteau Creek Hydroelectric Station at Gardiner Dam ~130 river km upstream. These transects were 200 m long and located within Saskatoon's city limits.

Including the reference site and the downstream reaches and boat launches, a total of 60 transect walks, representing 8198.5 m, were completed (Table 2). In Reach 1, 19 transects of an average length of 137 m were monitored once a month for six months (Tables 2, S3). In Reach 2, 19 transects of an average length of 119 m were monitored once a month for 5 months (Tables 2, S3). Finally, 18 transects with an average length of 141 m were monitored once a month for 5 months in Reach 3 (Tables 2, S3). Boat launch and Saskatoon transects were 200 m and monitored 6-times once a month over 6 months (Table 2).

2.4 | Habitat assessment

Substrate assessments were performed at the same time when camera mounts were deployed and the first transects were conducted in each reach. Larger substrates are believed to increase stranding risk because they provide cover for fish and less incentive to move in response to dewatering (Hauer, Unfer, Holzapfel, Haimann, & Habersack, 2014; Saltveit et al., 2001). Substrate was reassessed at locations where fish were found during transect monitoring, and if no fish were discovered, the original transect substrate was used. The substrate was assessed using a modified Wentworth scale; clay <0.004 mm, silt 0.004–0.06 mm, sand 0.06–2 mm, pebble 2–64 mm, cobble 64–256 mm and boulder >256 mm (Wentworth, 1922), assigning a percentage to each substrate type present within the 6.50–7.26 m^2 covered by the camera and the area covered by the transect. The

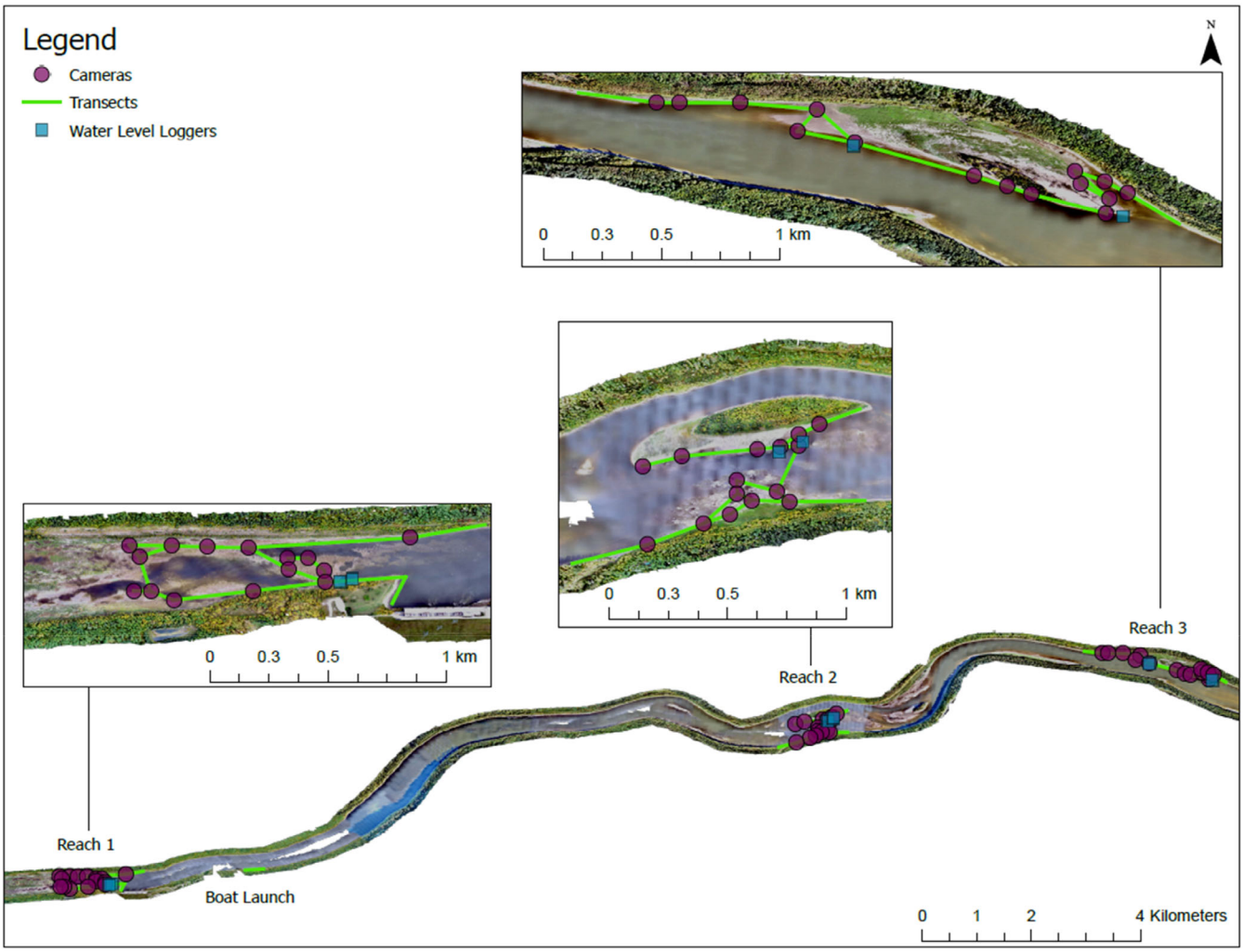

FIGURE 3 Reach 1, Reach 2, and Reach 3 downstream of the E.B. Campbell Hydroelectric Station in the Saskatchewan River. Camera mount locations are represented as purple circles, transects symbolized by green lines, and water level loggers represented as blue squares. [Color figure can be viewed at wileyonlinelibrary.com]

substrate composition for each camera and transect was determined by taking the percent of each substrate using mean substrate particle sizes (clay 0.002 mm, silt 0.032 mm, sand 1.3 mm, pebble 33 mm, cobble 160 mm and boulder 628 mm).

Four slope measurements were made at each camera mount after its installation using a construction level (125.73 cm in length). Measurements were in the following directions: orthogonal to the thalweg and towards the river bench, and upstream and downstream the river with respect to the camera mount, resulting in typically both positive and negative rises. The minimum rise was subtracted from the maximum rise to calculate the overall rise and then divided by the total of two runs (251.46 cm) to calculate the overall slope at each camera location. The slope was calculated using the absolute value of the rise over the run of both measurements. Slopes were not measured at the transect fish stranding locations. Consequently, the variable slope was not included in the model of the transect monitoring dataset.

Water level and temperature within the reaches were recorded with water level data loggers (Onset, U20L-01, Onset, Bourne, MA, USA) deployed at the upstream and downstream ends of each study reach (Figure 3). To account for barometric pressure changes, an additional logger was deployed in a dry location at Reach 1 to measure atmospheric pressure and allow for barometric correction of the water level data. All loggers were set to record pressure and temperature every 30 min.

Using the data from the water level logger, a reach specific vertical ramping rate ($cm \cdot h^{-1}$) was calculated for each 30 min interval. For Reaches 2 and 3, the mean vertical ramping rate of the upstream and downstream logger data was used for this analysis. However, due to the complex riverbed morphology in Reach 1, the 10 cameras situated in the upstream portion of Reach 1 characterized by a steeper riverbed, were associated with vertical ramping rates obtained from the upstream logger, whereas the remaining five cameras located in the downstream areas were associated with the vertical ramping rates of the downstream logger (Figure 3). Furthermore, the vertical ramping rate and slope were transformed to obtain a horizontal ramping rate for camera locations. The vertical ramping rate divided by the slope at

FIGURE 4 (a) Example of the mean ramping rate ($cm \cdot h^{-1}$) in Reaches 1, 2, and 3 obtained from water level data loggers that were deployed at the up- and downstream location of each reach from July 1–10, 2021; and (b) Discharge ($m^3 \cdot s^{-1}$) of the E.B. Campbell Hydroelectric Station from July 1–10, 2021 measured at the water gauge 05KD003, Canada Water Survey. [Color figure can be viewed at wileyonlinelibrary.com]

the respective camera determined the horizontal ramping rate for all recorded stranding possibilities.

As transect monitoring was typically conducted during daylight hours, after the flow had receded and fish stranding had occurred, the time of fish stranding could not be accurately determined. Therefore, for the transect monitoring dataset, we assumed that the time of the stranding event occurred at the highest magnitude of the down ramping rate. Consequently, the selected ramping rate was the maximum ramping rate since the previous low water level (Figure 4). The same time point was used for the water temperature associated with the fish stranding.

2.5 | Fish community sampling

Seine netting was conducted to determine what species and life stages were present in the study reaches during the study period, and therefore had the potential to strand. The fish sampling was performed with a 9.14 m × 1.82 m beach seine with a 4.76 mm mesh size and a 1.82 m^3 centre pocket. During each of the monthly visits, five seine hauls were conducted at each reach in the afternoons when flows were high. Seining was performed in a semi-circle by two people, with one person acting as the pivot and holding one side of the seine net while the other crew member extended the net along the shore, upstream from the pivot point and swept it out along the river margin following the direction of the flow (Bonar, Hubert, & Willis, 2009). The preformed seine radius was estimated to allow for calculation of area sampled, fully deployed seines sampled an ~8 m radius semi-circle (~100 m^2). Once the sweep was completed, both crew members pulled the lead and float lines together onto the shore, trapping the fish in the seine bag. Fish were then identified to species, counted and returned to the river, while one reference individual was collected per species and brought to the laboratory for confirmation of the species identification and length and body mass measurements.

2.6 | Image analysis

Fish stranding is dependent on the river channel being wet and then dry as the water level fluctuates with the changing flow releases from the hydroelectric station. At the three study reaches, the highest instantaneous discharge did not necessarily inundate each camera location on each day. For example, if the camera location was placed at a higher elevation than the water level reached by the highest instantaneous discharge, stranding could not have occurred that day because the location stayed dry. As well, a camera location set at the lower elevation was not always de-watered daily if the minimum flow maintained a water surface elevation that kept the camera location inundated. If a camera location went through a wet-dry-cycle, then this indicated that stranding was possible for that location, and we refer to each of these as a 'potential stranding event'. These events could occur across more than one day, as typically flows peaked in the evening and were at their minimum in the early morning (Figure 4).

All images from all camera locations for the deployment period were inspected for when a potential stranding event occurred, defined as when all water in the image lost connection with the thalweg. The time of the potential stranding event was identified from the date/time stamp on the time lapse camera image. The ramping rate and water temperature at this time point were then associated with the event. The total number of potential stranding events for each camera location, per study reach, was summarized. Several camera locations suffered failure due to environmental or wildlife interference; these time periods were excluded from the data analysis. Wetted history was determined as the period that water covered the area in view of the camera before an observed stranding possibility, calculated as the time difference between a dry image and the earliest preceding wet image.

Camera images following a potential stranding event were then examined for stranded fish. Images were processed by two observers for validation and data quality control. Any observed stranded fish was identified to species, if possible, and fish length was estimated through pixel counts using CellProfiler software (Cambridge, MA, USA). Fish length measured in pixels was subsequently converted to millimetres using the base of the camera mount pole (25 mm) as a reference. Fish length was then categorized into four size classes (Table S1).

When a stranded fish was observed, the subsequent images were inspected for scavenging by wildlife. Scavenging was assumed when stranded fish disappeared in the following images before the next water inundation occurred. The image taken after the fish disappeared was noted, and the scavenging time was calculated as the time period between fish stranding and scavenging.

2.7 | Data and statistical analyses

The fish stranding density (fish·m^{-2}) was calculated for both the remote photography and transect monitoring to allow for comparisons between the two methodologies. The cameras captured a surface area ranging from 6.50 to 7.26 m^2 of the riverbed in each image. The transect walk area was calculated by multiplying the total length of a given transect by 3 m (i.e., 1.5 m either side of the transect). Similarly, fish density (fish·m^{-2}) was calculated for fish seining efforts. The number of fish observed or collected from three methodologies (i.e., remote photography, transect monitoring, and seine netting) was then divided by the respective area covered. A t-test was performed using all fish stranding densities of remote photography and transect monitoring calculated for the entire study (Tables S2, S3) to analyse if the fish stranding densities were statistically different between the two methodologies.

Generalized linear models (GLM), fit with the GLM function in the R 2.10.0 package (R Development Core Team, 2010), were used to develop predictive models of fish stranding. Separate models were developed for the remote photography and the transect monitoring datasets. For the remote photography data, the model was developed using the calculated fish stranding densities as the response variable and the predictor variables were the horizontal ramping rate (cm·h^{-1}), water temperature (°C), substrate (mm) and wetted history (min) (Model 1).

Model 1 – Remote Photography

$$\begin{aligned}\text{Fish Stranding Density} = \text{glm}(&\log(\text{Fish Stranding Densities}+1)\\ &\sim \text{Horizontal Ramping Rate}\\ &+\text{Water Temperature}+\text{Substrate}\\ &+\text{Wetted History})\end{aligned}$$

The transect data model used fish stranding density as the response variable and the predictor variables were vertical ramping rate (cm·h^{-1}), water temperature (°C), and substrate type (mm) (Model 2).

Model 2 – Transect Monitoring

$$\begin{aligned}\text{Fish Stranding Density} = \text{glm}(&\log(\text{Fish Stranding Densities}+1)\\ &\sim \text{Vertical Ramping rate}\\ &+\text{Water Temperature}+\text{Substrate})\end{aligned}$$

The fish stranding densities used in both models were based on the effort of sampling, with remote photography densities calculated using each 'potential stranding event' as a unit of replication and transect monitoring densities calculated using each transect in each survey as a unit of replication.

Due to overdispersion, a quasi-Poisson regression was conducted to determine the deviances in the GLM model (Takahashi & Kurosawa, 2016). For each model variable, we tested if homoscedasticity of variance was met using Levene's test. If data transformation was needed, fish stranding density was log transformed to reduce heteroscedasticity. Additional assumption testing was conducted by running the model as a logistic regression (where the response variable was either stranding or no stranding) to compare against the model with log transformed fish stranding density data. A generalized linear

mixed model (GLMM) was performed with the random effects of reach and camera/transect location, but issues around model convergence and limited variation meant we were unable to run this more complex model, so the random effects were removed and the model re-analysed.

3 | RESULTS

3.1 | Fish stranding downstream of E.B. campbell hydroelectric station

Remote photography using time lapse cameras captured a total of 59 stranded fish within the images over the deployment period. Fifty-eight of the fish observed by the cameras were size class 1 (young-of-the-year), while only one fish was size class 4 (large). Species identification was not reliable for young-of-the-year fish (Figure 5). A total of nine fish were observed stranded in Reach 1 by the 15 cameras deployed for 149–151 days (d) (Table 1). In Reach 2, 15 cameras were deployed for 121–122 d observing a total of 24 stranded fish (Table 1). Finally, in Reach 3, 15 cameras deployed for 117–118 d observed a total of 26 stranded fish (Table 1). All cameras combined, a total of 651 d of observational time was missed due to camera failures (Table S2). The highest number of stranded fish was observed in July, with a total of 38 individuals across all three reaches combined. Reach 2 had the highest fish stranding density with 0.0042 fish·m^{-2} (Table 1).

Out of the 59 stranded fish, 32 were estimated to be scavenged. Average time until removal occurred was 240 min, with a minimum time of 30 min and a maximum time of 780 min (Figure S2). The remaining 27 fish were inundated by water during the next hydropeaking event and scavenging was therefore not observed.

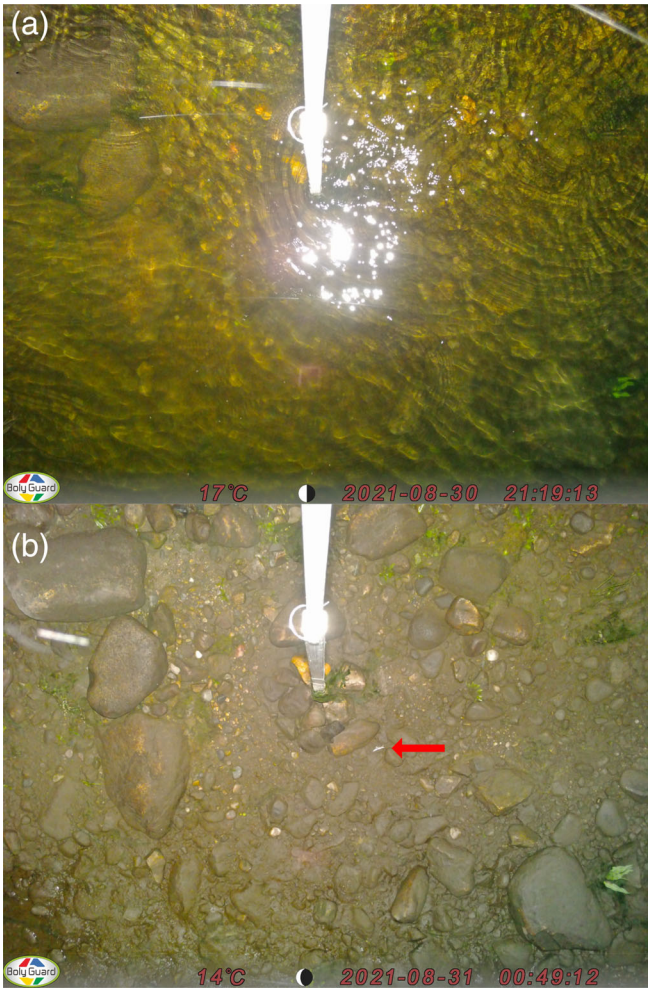

FIGURE 5 Example images of trail cameras capturing images of the riverbed. (a) Image representing water coverage allowing habitat accessibility, taken at 21:19:12 on August 8th, 2021. (b) Image representing water recession exposing a stranded fish, taken at 00:49:12 on August 8th, 2021. The stranded fish species, located in the centre of image B and indicated by the arrow, was not identifiable. [Color figure can be viewed at wileyonlinelibrary.com]

3.2 | Fish stranding composition

During transect monitoring, a total of 2,343 stranded fish were found, representing 15 species; 1,021 of these fish were discovered alive, lying on the dry riverbed or in isolated pools that were not survivable to the next water inundation, and 1,322 were dead. Fish were located at 116 different coordinates within 36 transects out of a total of 323 transects conducted during the study period. The largest number of fish discovered in one location (N 53.726117 W 103.177737) was 809 on July 17, 2021. The most common species that stranded was the white sucker (*Catostomus commersonii*), with 1,627 individuals (Table 4). A total of 270 fish were collected at Reach 1, 297 fish at Reach 2, 1,742 fish at Reach 3, 34 fish at the first boat launch, and zero fish during the transect monitoring at the second boat launch and in Saskatoon (Table S4). The highest number of fish stranded was in Reach 3 with 1,742 fish over the study period, and the fish stranding density was highest in Reach 3 with 0.0457 fish·m^{-2} (Table 2). During transect monitoring, 2,302 young-of-the year (size class 1) fish, 32 small (size class 2) fish, 6 medium (size class 3) fish, and 2 large (size class 4) fish were observed (Table 4).

A total of 7,246 fish, representing 11 species, were caught in the seine net surveys (Table 4). The most abundant species was the emerald shiner (*Notropis atherinoides*), with a total of 2,823 individuals caught over the study period (Figure 6). The highest fish density from seine netting was at Reach 1 (Table S4). The greatest fish density was found at Reach 1 with 1.6453 fish·m^{-2} (Table 3).

3.3 | Comparing methodologies

When comparing remote photography and transect monitoring, though occasional high density stranding events were observed on transects (Figure 7), there was a minimally significant difference in fish stranding density between methods ($t = -2.04$, $df = 56.23$, p-value $= 0.046$). Figure 7 shows that the fish stranding densities of

TABLE 1 Fish stranding density during the collective efforts of remote photography

Location	Number of cameras	Cumulative operational days	Camera failures days	Stranding possibilities	Total area surveyed (m^2)	Number of stranded fish	Fish stranding density ($fish \cdot m^{-2}$)
Reach 1	15	2249	240	1308	9256.9	9	0.0010 ± 0.003
Reach 2	15	1828	169	859	6236.3	24	0.0038 ± 0.005
Reach 3	14	1646	242	1045	7586.7	26	0.0034 ± 0.004

TABLE 2 Fish stranding density during the collective efforts of transect monitoring

Location	Number of transects	Observing days	Total area of view in each survey (m^2)	Total area surveyed (m^2)	Number of fish found	Fish stranding density ($fish \cdot m^{-2}$)
Reach 1	19	6	7817	46904	270	0.0058 ± 0.02
Reach 2	19	5	6761	31997	297	0.0093 ± 0.02
Reach 3	18	5	7618	38088	1742	0.0457 ± 0.06
Boat Launch 1	1	6	600	3600	34	0.0047 ± 0.01
Boat Launch 2	1	6	600	3600	0	0
Saskatoon	2	6	1200	7200	0	0

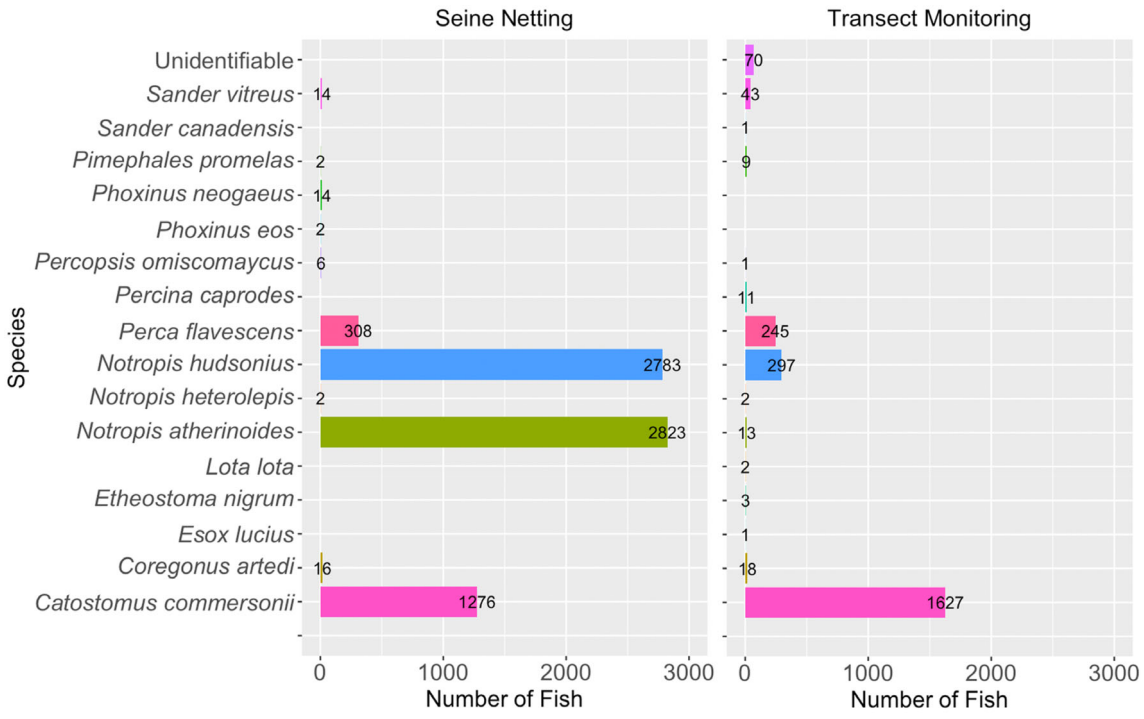

FIGURE 6 Number of fish per species caught in seine netting surveys representing the local fish community that is subject to stranding compared to the number of stranded fish observed during transect monitoring. [Color figure can be viewed at wileyonlinelibrary.com]

each method are comparable as they overlap in ranges for each respective reach. Therefore, the two methodologies provide comparable fish stranding densities.

3.4 | Fish stranding modelling

Heteroscedasticity in the variance was found for multiple variables within both datasets. Subsequently, the raw data was log transformed to reduce heteroscedasticity (due to a high volume of zero values, a value of one was added to all datapoints before log transformation). The logistic regression model showed similar patterns as the GLM models with log-transformed data, so the log-transformed GLM models are presented here. There is reduced statistical power in our model for remote photography as there are only 59 data points where stranded fish were observed and a large number of zero values for the response variable.

Model fitting of data obtained by remote photography resulted in a positive relationship between fish stranding density and water

TABLE 3 Fish density during the collective efforts of fish sampling using a seine net

Location	Total area seined (m^2)	Number of fish caught	Fish density ($fish \cdot m^{-2}$)
Reach 1	2532	4452	1.6453 ± 6.3
Reach 2	2221	834	0.5444 ± 2.0
Reach 3	2341	1960	0.8631 ± 2.8

TABLE 4 Species collected during seine netting and transect monitoring. The numbers are summarized by size class (1 – young-of-the-year, 2 – small, 3 – medium and 4 – large (Table S1)).

	Seine netting			Transect monitoring				
Species collected	Size 1	Size 2	Seine total	Size 1	Size 2	Size 3	Size 4	Transect total
blacknose shiner	2		2	2				2
burbot				1	1			2
cisco	16		16	6	12			18
emerald shiner	2822	1	2823	7	2	3	1	13
fathead minnow	2		2	8	1			9
finescale dace	12	2	14					
johnny darter				2	1			3
logperch					10		1	11
northern pike				1				1
northern redbelly dace	2		2					
Sauger				1				1
spottail shiner	2783		2783	292	3	2		297
troutperch	6		6	1				1
unidentifiable				70				70
walleye	14		14	42	1			43
white sucker	1276		1276	1624	2	1		1627
yellow perch	227	81	308	245				245
Grand Total	7162	84	7246	2303	32	6	2	2343

temperature (Table 5; Figure 8). There was a negative relationship between fish stranding density and substrate (Table 5; Figure 8); smaller particle sizes were associated with higher fish stranding densities. Horizontal ramping and wetted history had no significant effect on fish stranding density (Table 5).

The transect monitoring data model revealed an increase of fish stranding density with increasing water temperature (Table 6; Figure 9). In addition, the density of stranded fish increased with smaller particle sized substrates (Table 6; Figure 9). There was no effect of vertical ramping rate on fish stranding density.

4 | DISCUSSION

Our assessment of fish stranding risk downstream of the E.B. Campbell Hydroelectric Station used an innovative remote photography approach. By taking a picture every 30 min for a five-month period, we were able to document the stranding potential in three downstream reaches. Our cameras were placed in locations where there was a stranding risk for more than half of the observational period at all three reaches, highlighting the spatial and temporal extent of the influence of the hydropeaking regime of the station. The hydropeaking regime is unlike a natural river and is theoretically beyond the abilities of species occupying the river to adapt and quickly move away as areas dewater during down-ramping. The channel morphology in the three study reaches is such that vertical ramping rates are greatest below the powerhouse, but horizontal ramping rates are greatest in reaches 2 and 3 (Figure S3), where a greater number of stranded fish were discovered. Hydropeaking is known to impact the Saskatchewan River's water surface elevation for ~60 km downstream, indicating fish stranding could occur over this entire distance. This suggests that the entire fish community structure is being affected in the ~60 km downstream reach and indicates there are more variables influencing fish stranding than just the hydropeaking regime, such as water temperature, substrate, fish life history and body size.

In the drainage near the study reaches, there are ~37 fish species. In the seine netting surveys, we observed a total of 11 species in the

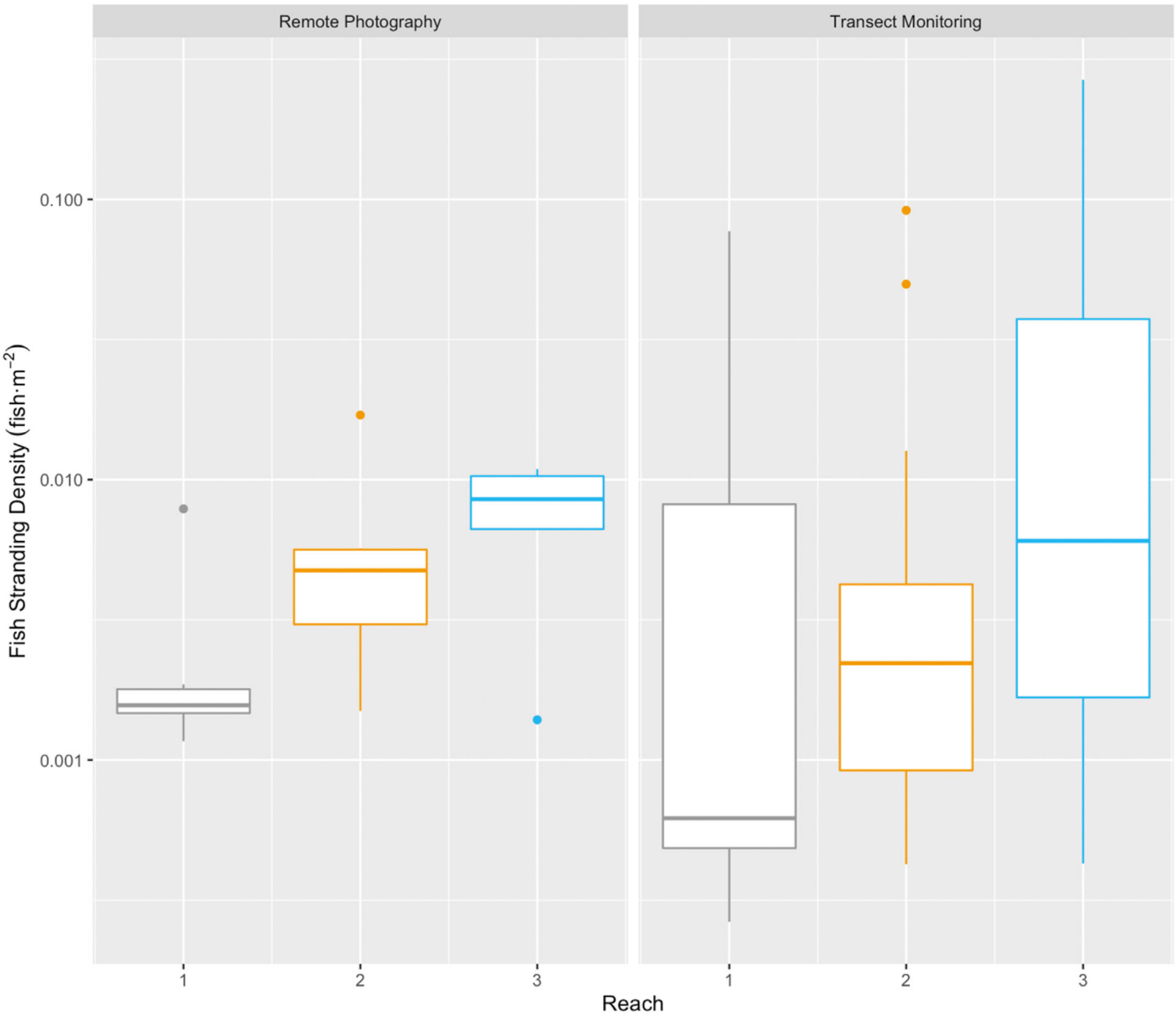

FIGURE 7 Comparison of all calculated fish stranding densities (fish·m^{-2}) from remote photography and transect monitoring. Y-axis is on a logarithmic scale. [Color figure can be viewed at wileyonlinelibrary.com]

Predictor variables	Estimate	Standard error	T-value	*p*
Horizontal ramping rate	7.11×10^{-6}	2.739×10^{-5}	0.26	0.795
Water temperature	3.49×10^{-3}	1.41×10^{-3}	2.47	0.014
Substrate	-9.05×10^{-5}	3.78×10^{-5}	−2.40	0.017
Wetted history	-1.94×10^{-5}	1.67×10^{-5}	−1.16	0.246

TABLE 5 GLM results for remote photography model with fish stranding density (fish·m^{-2}) as the response variable and the predictor variables, horizontal ramping rate, water temperature, substrate type, and wetted history.

three study reaches, compared to the 15 species observed during transect monitoring. Remote photography observed a northern pike (*Esox lucius*), and a burbot (*Lota lota*), but other stranded fish were not identifiable (Figure 5). The image quality does not allow distinguishing small features required for species identification, especially as the majority of stranded fish captured in the images were small bodied, young-of-the-year fish. Stranding susceptibility is likely different based on a species habitat selection and behaviour, as some species, for example, the emerald shiner, spottail shiner (*Notropis hudsonius*), trout-perch (*Percopsis omiscomaycus*), stranded less than expected based on their proportion in the seine net catch (Figure 6). Juvenile sport and commercial fish species, for example, walleye (*Sander vitreus*), white sucker, yellow perch (*Perca flavescens*), cisco (*Coregonus artedi*), burbot and northern pike stranded more often based on their proportion in the seine net catch (Figure 6), but we have no explanation for this finding based on physiology or behaviour. This could be a

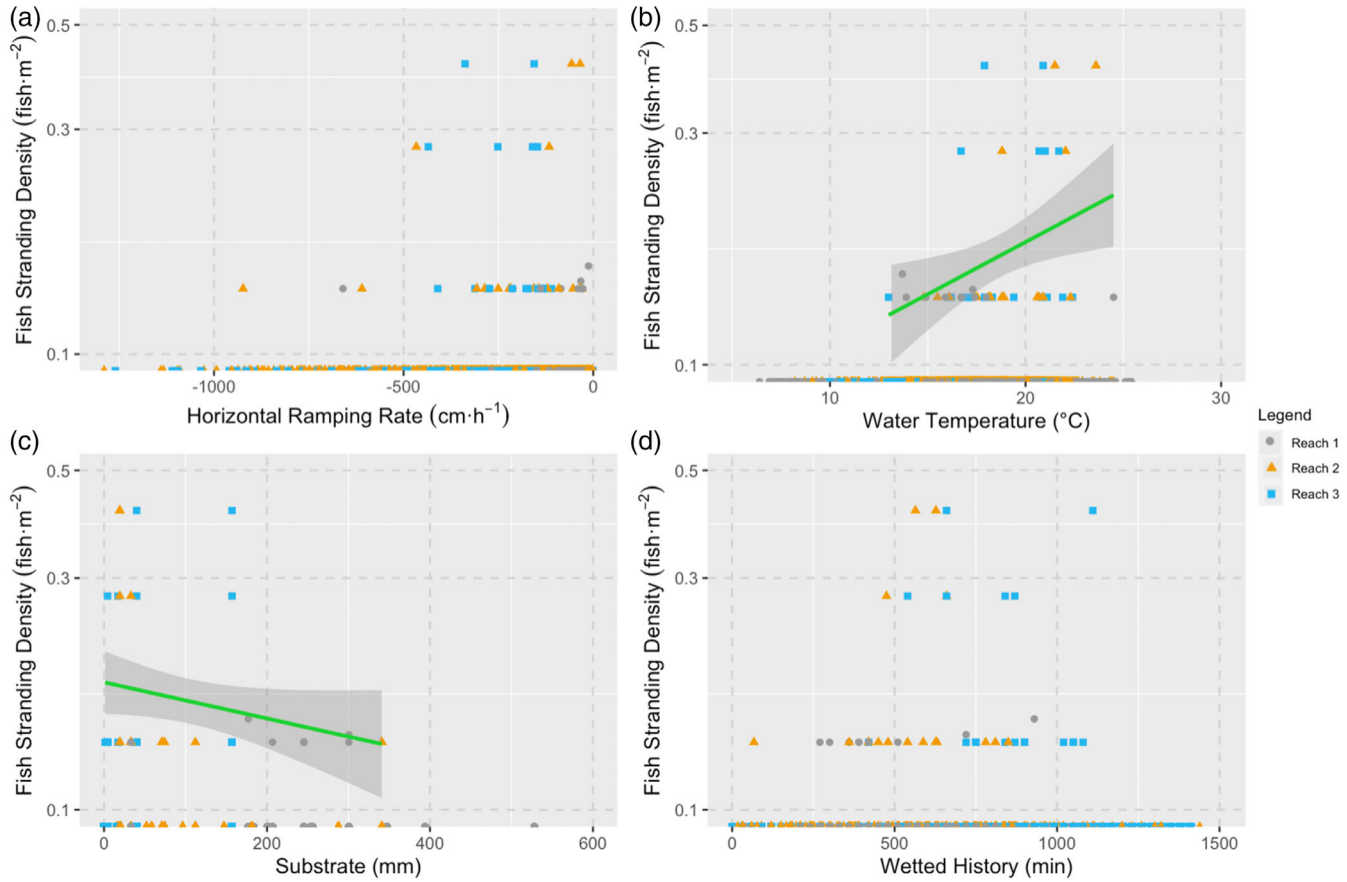

FIGURE 8 Fit of the model for the response variable fish stranding density (fish·m^{-2}) observed using remote photography with respect to the predictor variables (a) horizontal ramping rate (cm·h^{-1}), (b) water temperature (°C), (c) substrate type (mm), and (d) wetted history (min). Variables with significant relationships have a trendline to represent the relationship between variables. Each data point represents a "potential stranding event" as a unit of replication. Y-axis is on a logarithmic scale and many of the data points are superimposed. [Color figure can be viewed at wileyonlinelibrary.com]

TABLE 6 GLM results for transect monitoring model with fish stranding density (fish·m^{-2}) as the response variable and the predictor variables, vertical ramping rate, water temperature, and substrate type.

Predictor variables	Estimate	Standard error	T-value	*p* value
Vertical ramping rate	−0.007	0.013	−0.567	0.57
Water temperature	0.265	0.044	5.975	<0.001
Substrate	−0.003	0.001	−3.829	<0.001

result of habitat and/or behavioural adaptation leading to increased stranding risk. Alongside juvenile sport and commercial fish species, other species were not caught in the seine net but were subject to stranding. For example, burbot are more sedentary during daylight hours when seining occurred, becoming more active during the night (McPhail & Paragamian, 2000) when the hydropeaking regime subjects them to potential stranding. Accordingly, we did not catch any burbot in seine netting, but the species was observed during transect monitoring in the morning after the water level fell overnight, as was the case for johnny darter (*Etheostoma nigrum*), logperch (*Percina caprodes*), northern pike, and sauger (*Sander canadensis*). In addition, lake sturgeon (*Acipenser fulvescens*) are known to occupy the river (Abu, 2020; Enders et al., 2017) but were never seen to be stranded or in fish sampling. This is likely due to gear selectivity.

The highest proportion of stranded fish was composed of juvenile and small-bodied fish. Juvenile and small-bodied fish are more likely to use the nearshore habitat due to the available food resources, flow refugia, and habitat structure providing shelter from predators (Irvine et al., 2015). Juvenile fish are known to be slow to move away from nearshore areas when water levels decrease (Korman & Campana, 2009), putting them at a higher risk of stranding compared to adults. During the May survey, young-of-the-year emerald shiner dominated the catch in the seine netting, but emerald shiner were neither seen in large numbers in later study months in the seine netting nor during transect monitoring (Table S5), when stranding rates for all species combined were the highest. Likely, emerald shiner habitat selection and behaviour reduced their stranding risk.

Despite the advantages of remote photography, there were some complications using the camera mounts. For example, in a substrate dominated by boulders and cobble, the camera mounts could not be

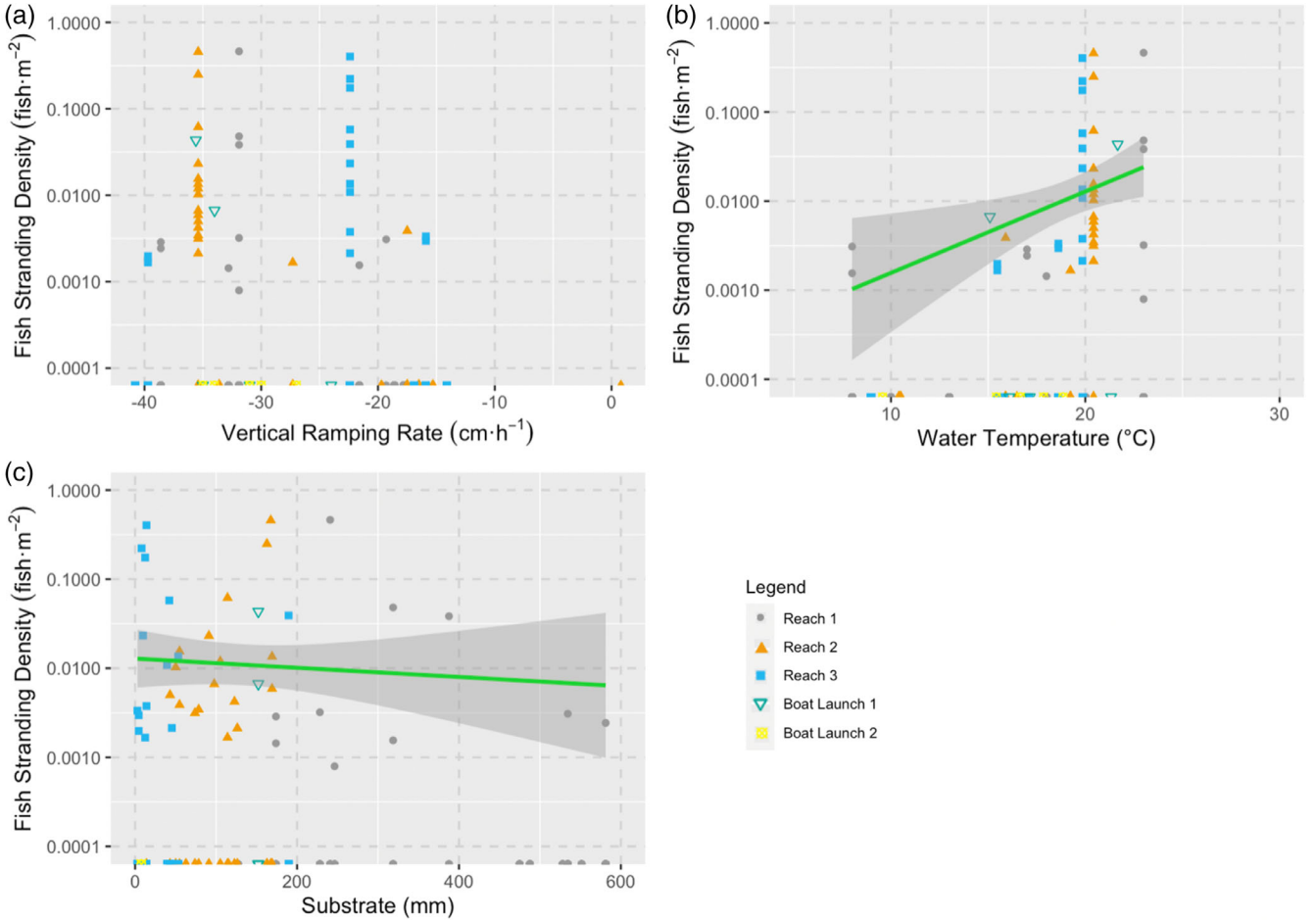

FIGURE 9 Fit of the model for the response variable fish stranding density (fish·m^{-2}) observed using during transect monitoring with respect to the predictor variables (a) vertical ramping rate (cm·h^{-1}), (b) water temperature (°C), and (c) substrate type (mm). Variables with significant relationships have a trendline to represent the relationship between variables. Each data point represents a transect survey as a unit of replication. Y-axis is on a logarithmic scale and many of the data points are superimposed. [Color figure can be viewed at wileyonlinelibrary.com]

buried into the substrate, which made these mounts vulnerable to being pushed over by wildlife or unfavourable weather conditions (i.e., strong wind). The study year also had lower than average discharge, so we are uncertain whether the mounts would hold against significant flooding. Wildlife was attracted to the camera mounts and were frequently observed in images and during site visits. Eagles and small birds used them as perches. Coyotes were curious about the tie ropes and chewed and cut multiple ropes during the study period. Arachnids used the mounts to support their webs, which were frequently seen in the images and sometimes obscured the view of the camera. Subsequently, we recommend that camera mounts are frequently maintained to assure full functioning.

Transect monitoring depends on the availability of field staff, is time intensive, and often allows for only sporadic observations. During transect monitoring, large numbers of fish that stranded in the same area were discovered, reflecting the often-clustered nature of stranding events. Due to the patchy nature of the fish stranding and fish occurrence in general and the larger surface area surveyed during transect monitoring, a higher absolute number of fish were observed during transect monitoring, but the relative fish stranding density between the two methods is comparable.

Remote photography captured stranding events as flows dropped during the night; our sample period used for modelling summarized these events to within 30 min of the occurrence. In contrast, our transect monitoring was conducted after the fish stranding occurred, possibly after scavenging had happened. More than half of the fish observed stranded by the remote photography were scavenged on average 240 min after the water receded. Therefore, it is possible that when small numbers of fish strand in a location, similar to the numbers observed in the remote photography, a large proportion of them may have been scavenged before the transect monitoring was conducted. This would result in an underestimation of the fish stranding for the transect monitoring. Stranding occurred as the flows typically decreased between 18:00 h and 6:00 h when it was dark, but the timing varied from day to day. Therefore, the ramping rate for the transects was an estimate, not necessarily specific to when the stranding occurred.

An additional limitation of observing fish with remote photography or during the transect monitoring is the substrate particle size. Large particle sizes create interstitial spaces. If fish are in these interstitial spaces, they might not be visible using either method. During transect monitoring, fish were seen in crevasses created by large

boulders and cobble; however, the observers' ability to change the angle of their viewpoint should have observed more fish than the remote photography.

Remote photography provides advantages due to the continued surveying ability and relation to stranding parameters. Though there was no significant difference in the ability of the methodologies to capture fish stranding densities, transect monitoring was beneficial in capturing a greater sample size of stranded fish used to understand species being stranded. It is suggested that remote photography mounts are continually checked throughout a study period to reduce complications from weather and wildlife, and on-site transects should be conducted in a timely manner as soon as possible after water levels drop to minimize fish lost to scavenging. To best depict the extent of fish stranding, a combination of remote photography and transect monitoring is recommended.

In the temperature range of 6–25°C, we observed a positive relationship between fish stranding density and water temperature. Water temperature affects fish behaviour and metabolism (Korman & Campana, 2009). For example, warmer nearshore habitat may attract juvenile fish to optimize growth (Korman & Campana, 2009), resulting in an increased stranding risk. Additional studies are needed to explore fish stranding during the winter months, as ice cover periods are important for understanding how fish occupy the river habitat (Linnansaari et al., 2009). In general, at colder water temperatures, a higher stranding risk is observed (Irvine et al., 2009; Juárez, Adeva-Bustos, Alfredsen, & Dønnum, 2019; Puffer et al., 2015; Saltveit et al., 2001) as the fish's swimming capacity decreases (Canal, Laffaille, Gilbert, Lauzeral, & Buisson, 2015). In addition, during the winter season, under colder water temperatures, the fish become more sedentary, which can also result in an increased potential for stranding (Scruton et al., 2005). While the sedentary behaviour of fish during the winter is a response to conserve energy reserves, hydropeaking may increase stress levels and energy demands in fish (Scruton et al., 2005).

The GLM models revealed relationships between the fish stranding density and the type of substrate. The models showed that finer substrates, such as silt and sand, were associated with an increase in fish stranding. Continuous change in substrate distribution occurs as the water levels rise and fall, creating pools or potholes in sandy areas that are stranding hotspots (Irvine et al., 2009; Moreira, Schletterer, Quaresma, Boavida, & Pinheiro, 2020; Tuhtan, Noack, & Wieprecht, 2012). Pools and potholes near the shore allow the fish to congregate in shallow areas and get trapped in areas away from the thalweg, increasing the chance of stranding (Auer et al., 2017; Irvine et al., 2009). During transect monitoring, stranded fish were commonly found in patches that occurred in potholes formed in the substrate, most common on sand. This was also witnessed in remote photography; as water levels receded, fish congregated in pools and potholes that disconnected from the thalweg and then became stranded as the water retreated. However, previous studies have determined that there is high variability in predicting fish stranding based on substrate (Hauer et al., 2014), and our models were complicated by the interplay between spatial (substrate) and temporal (temperature) effects, which likely interact. More data with a greater number of stranding observations would help develop more robust models.

Although we did not find a relationship between horizontal or vertical ramping rates and stranding, we know stranding can only occur when water levels recede. A lack of relationship in horizontal and vertical ramping rates could be a result of the sporadic nature of the station's hydropeaking and insufficient data to define an association with a small range of horizontal and vertical ramping rates represented. Previous studies showed that stranded fish are more commonly observed in river reaches with gradual riverbanks with a greater horizontal ramping rate, as slower water velocities create optimal habitat for juvenile and small-bodied fish (Irvine et al., 2015; Tuhtan et al., 2012), exposing them to increased stranding potential. In addition, there was no supporting evidence for effects of wetted history, although the wetted history could also affect the stranding potential. Irvine et al. (2015) found that with an increased wetted history, there is an increased risk of fish stranding due to additional cover or forage availability leading to more fish choosing to occupy the nearshore environment. Stranding data distributions have a large number of zeroes, creating challenges for building robust models. Consequently, further studies are required to further investigate the mechanism between these variables and fish stranding.

In conclusion, our study demonstrated that the hydropeaking of the E. B. Campbell Hydroelectric Station can lead to the mortality of juvenile and small-bodied fish. Enders et al. (2017) noted lower densities of juvenile and small-bodied fish downstream from the station in comparison to an unaffected upstream site, and our results indicate that fish stranding may be a contributing factor to the lower numbers of these life stages and fish species. In addition, since the installation of the hydroelectric station, there has been a decline in fish populations downstream in the Saskatchewan River Delta (Abu et al., 2020). Our results showed that water temperature and substrate affect stranding risk, but surprisingly, horizontal ramping rate or wetted history did not have a significant effect, even though these variables are known to influence stranding risk elsewhere (Irvine et al., 2009, 2015; Nagrodski et al., 2012; Young, Cech, & Thompson, 2011). Based on our results, minimizing the hydroelectric station's hydropeaking during periods of warmer water temperatures could reduce the number of stranded fish. Additional use of remote photography and transect monitoring should occur to study fish stranding further downstream on the Saskatchewan River and in other river systems, to observe fish stranding in colder periods, and to validate the fish stranding model results. The use of remote photography has been proven to be a valuable methodology that can be applied to hydropeaking rivers globally to gain a better understanding of fish stranding.

ACKNOWLEDGEMENTS

This study was financially supported by Fisheries and Oceans Canada's Freshwater Habitat Science Initiative (FHIN). We would like to thank Andrea Kneale, Colin Kovachik, Adam Waterer, Stefanie Kornberger, Holly Simpson, Monica Giesbrecht, Nici Schaefer, Michela Carriere, Michaella Barnes, David Braun, Kayla Gagliardi, Robert

Barrett, Ramona Muster and Ryann Teillet for their assistance in field data collection, sample analysis in the lab, and image processing, and Nicolas Lamouroux and an anonymous reviewer for their comments that greatly improved the paper.

DATA AVAILABILITY STATEMENT

The data that support the findings of this study are available from the corresponding author, Sarah E. Glowa, upon reasonable request.

ORCID

Sarah E. Glowa https://orcid.org/0000-0002-0711-6642
Timothy D. Jardine https://orcid.org/0000-0002-5917-9792

REFERENCES

Abu, R., Reed, M. G., & Jardine, T. D. (2020). Using two-eyed seeing to bridge Western science and Indigenous knowledge systems and understand long-term change in the Saskatchewan River Delta, Canada. *International Journal of Water Resources Development*, *36*(5), 757–776. https://doi.org/10.1080/07900627.2018.1558050

Algera, D. A., Rytwinski, T., Taylor, J. J., Bennett, J. R., Smokorowski, K. E., Harrison, P. M., … Cooke, S. J. (2020). What are the relative risks of mortality and injury for fish during downstream passage at hydroelectric dams in temperate regions? A systematic review. *Environmental Evidence*, *9*(1), 1–36. https://doi.org/10.1186/S13750-020-0184-0/FIGURES/17

Auer, S., Zeiringer, B., Führer, S., Tonolla, D., & Schmutz, S. (2017). Effects of river bank heterogeneity and time of day on drift and stranding of juvenile European grayling (*Thymallus thymallus L.*) caused by hydropeaking. *Science of the Total Environment*, *575*, 1515–1521. https://doi.org/10.1016/j.scitotenv.2016.10.029

Baston D. (2021). exactextractr: Fast Extraction from Raster Datasets using Polygons. R package version 0.7.2. https://CRAN.R-project.org/package=exactextractr

Bivand, R., Keitt, T., and Rowlingson, B. (2021). rgdal: Bindings for the 'Geospatial' Data Abstraction Library. R package version 1.5-27. https://CRAN.R-project.org/package=rgdal

Bivand R., and Rundel C. (2021). rgeos: Interface to Geometry Engine-Open Source ('GEOS'). R package version 0.5-8. https://CRAN.R-project.org/package=rgeos

Bonar, S. A., Hubert, W. A., & Willis, D. W. (2009). *Standard methods for sampling North American freshwater fishes*. Bethesda, MD: American Fisheries Society. http://pubs.er.usgs.gov/publication/70046706

Bradford, M. J. (1997). An experimental study of stranding of juvenile salmonids on gravel bars and in sidechannels during rapid flow decreases. *Ltd. Regulated Rivers Research & Management*, *13*, 395–401. https://doi.org/10.1002/(SICI)1099-1646(199709/10)13:5

Bruder, A., Tonolla, D., Schweizer, S. P., Vollenweider, S., Langhans, S. D., & Wüest, A. (2016). A conceptual framework for hydropeaking mitigation. *Science of the Total Environment*, *568*, 1204–1212. https://doi.org/10.1016/J.SCITOTENV.2016.05.032

Canal, J., Laffaille, P., Gilbert, F., Lauzeral, C., & Buisson, L. (2015). Influence of temperature on surface sediment disturbance by freshwater fish: a microcosm experiment. *International Journal of Limnology*, *51*(2), 179–188. https://doi.org/10.1051/LIMN/2015012

Cutler, T. L., & Swann, D. E. (1999). Using remote photography in wildlife ecology: A review. *Wildlife Society Bulletin*, *27*(3), 571–581.

Enders, E. C., Charles, C., Watkinson, D. A., Kovachik, C., Leroux, D. R., Hansen, H., & Pegg, M. A. (2019). Analysing Habitat Connectivity and Home Ranges of Bigmouth Buffalo and Channel Catfish Using a Large-Scale Acoustic Receiver Network. *Sustainability*, *11*(11), 3051. https://doi.org/10.3390/SU11113051

Enders, E. C., Watkinson, D. A., Ghamry, H., Mills, K. H., & Franzin, W. G. (2017). Fish age and size distributions and species composition in a large, hydropeaking Prairie River. *River Research and Applications*, *33*(8), 1246–1256. https://doi.org/10.1002/rra.3173

Eppehimer, D. E., Enger, B. J., Ebenal, A. E., Rocha, E. P., & Bogan, M. T. (2021). Daily flow intermittence in an effluent-dependent river: Impacts of flow duration and recession rate on fish stranding. *River Research and Applications*, *37*(10), 1376–1385. https://doi.org/10.1002/RRA.3850

Fisk, J. M., Kwak, T. J., Heise, R. J., & Sessions, F. W. (2013). Redd dewatering effects on hatching and larval survival of the robust redhorse. *River Research and Applications*, *29*(5), 574–581. https://doi.org/10.1002/RRA.2561

Flodmark, L. E. W., Urke, H. A., Halleraker, J. H., Arnekleiv, J. v., Vøllestad, L. A., & Poléo, A. B. S. (2002). Cortisol and glucose responses in juvenile brown trout subjected to a fluctuating flow regime in an artificial stream. *Journal of Fish Biology*, *60*(1), 238–248. https://doi.org/10.1111/J.1095-8649.2002.TB02401.X

Green, D. J., Jardine, T. D., Weber, L. P., & Janz, D. M. (2020). Energy stores and mercury concentrations in a common minnow (spottail shiner, *Notropis hudsonius*) associated with a peaking hydroelectric dam. *River Research and Applications*, *36*(7), 1046–1055. https://doi.org/10.1002/rra.3625

Guisández, I., Pérez-Díaz, J. I., & Wilhelmi, J. R. (2013). Assessment of the economic impact of environmental constraints on annual hydropower plant operation. *Energy Policy*, *61*, 1332–1343. https://doi.org/10.1016/J.ENPOL.2013.05.104

Hauer, C., Unfer, G., Holzapfel, P., Haimann, M., & Habersack, H. (2014). Impact of channel bar form and grain size variability on estimated stranding risk of juvenile brown trout during hydropeaking. *Earth Surface Processes and Landforms*, *39*(12), 1622–1641. https://doi.org/10.1002/ESP.3552

Irvine, R. L., Oussoren, T., Baxter, J. S., & Schmidt, D. C. (2009). The effects of flow reduction rates on fish stranding in British Columbia, Canada. *River Research and Applications*, *25*(4), 405–415. https://doi.org/10.1002/RRA.1172

Irvine, R. L., Thorley, J. L., Westcott, R., Schmidt, D., & Derosa, D. (2015). Why do fish strand? An analysis of ten years of flow reduction monitoring data from the Columbia and Kootenay rivers, Canada. *River Research and Applications*, *31*(10), 1242–1250. https://doi.org/10.1002/RRA.2823

Juárez, A., Adeva-Bustos, A., Alfredsen, K., & Dønnum, B. O. (2019). Performance of a two-dimensional hydraulic model for the evaluation of stranding areas and characterization of rapid fluctuations in hydropeaking rivers. *Water (Switzerland)*, *11*(2), 1–26. https://doi.org/10.3390/w11020201

Korman, J., & Campana, S. E. (2009). Effects of Hydropeaking on Nearshore Habitat Use and Growth of Age-0 Rainbow Trout in a Large Regulated River. *Transactions of the American Fisheries Society*, *138*(1), 76–87. https://doi.org/10.1577/t08-026.1

Larrieu, K. G., & Pasternack, G. B. (2021). Automated analysis of lateral river connectivity and fish stranding risks. Part 2: Juvenile Chinook salmon stranding at a river rehabilitation site. *Ecohydrology*, *14*(6), e2303. https://doi.org/10.1002/ECO.2303

Larrieu, K. G., Pasternack, G. B., & Schwindt, S. (2021). Automated analysis of lateral river connectivity and fish stranding risks—Part 1: Review, theory and algorithm. *Ecohydrology*, *14*(2), 1–11. https://doi.org/10.1002/eco.2268

Linnansaari, T., Alfredsen, K., Stickler, M., Arnekleiv, J. V., Harby, A., & Cunjak, R. A. (2009). Does ice matter? site fidelity and movements by Atlantic salmon (*Salmo salar l.*) parr during winter in a substrate enhanced river reach. *River Research and Applications*, *25*(6), 773–787. https://doi.org/10.1002/rra.1190

McPhail, D., & Paragamian, V. (2000). *Burbot Biology And Life History* (pp. 11–23). Bethesda, MD: American Fisheries Society, Fisheries Management Section.

Moog, O. (1994). Quantification of daily peak hydropower effects on aquatic fauna and management to minimize environmental impacts. *Biological Conservation*, *67*(2), 188–189. https://doi.org/10.1016/0006-3207(94)90377-8

Moore, K. M. S., & Gregory, S.v. (2011). Summer Habitat Utilization and Ecology of Cutthroat Trout Fry (*Salmo clarki*) in Cascade Mountain Streams, *45*(11), 1921–1930. https://doi.org/10.1139/F88-224

Moreira, M., Schletterer, M., Quaresma, A., Boavida, I., & Pinheiro, A. (2020). New insights into hydropeaking mitigation assessment from a diversion hydropower plant: The GKI project (Tyrol, Austria). *Ecological Engineering*, *158*. 1–14. https://doi.org/10.1016/j.ecoleng.2020.106035

Nagrodski, A., Raby, G. D., Hasler, C. T., Taylor, M. K., & Cooke, S. J. (2012). Fish stranding in freshwater systems: Sources, consequences, and mitigation. *Journal of Environmental Management*, *103*, 133–141. https://doi.org/10.1016/J.JENVMAN.2012.03.007

Puffer, M., Berg, O. K., Huusko, A., Vehanen, T., Forseth, T., & Einum, S. (2015). Seasonal Effects of Hydropeaking on Growth, Energetics and Movement of Juvenile Atlantic Salmon (*Salmo Salar*). *River Research and Applications*, *31*(9), 1101–1108. https://doi.org/10.1002/rra.2801

Rosenberg, D. M., McCully, P., & Pringle, C. M. (2000). Global-Scale Environmental Effects of Hydrological Alterations: Introduction. *Bioscience*, *50*(9), 746–751. https://doi.org/10.1641/0006-3568(2000)050[0746:gseeoh]2.0.co;2

RStudio Team. (2020). *RStudio: Integrated Development for R. RStudio*. Boston, MA: PBC. http://www.rstudio.com/

Saltveit, S. J., Halleraker, J. H., Arnekleiv, J.v., & Harby, A. (2001). Field experiments on stranding in juvenile atlantic salmon (*Salmo salar*) and brown trout (*Salmo trutta*) during rapid flow decreases caused by hydropeaking. *Regulated Rivers: Research & Management*, *17*(4–5), 609–622. https://doi.org/10.1002/RRR.652

Scruton, D. A., Pennell, C. J., Robertson, M. J., Ollerhead, L. M. N., Clarke, K. D., Alfredsen, K., … McKinley, R. S. (2005). Seasonal Response of Juvenile Atlantic Salmon to Experimental Hydropeaking Power Generation in Newfoundland, Canada. *North American Journal of Fisheries Management*, *25*(3), 964–974. https://doi.org/10.1577/m04-133.1

Silva, A. T., Lucas, M. C., Castro-Santos, T., Katopodis, C., Baumgartner, L. J., Thiem, J. D., … Cooke, S. J. (2018). The future of fish passage science, engineering, and practice. *Fish and Fisheries*, *19*(2), 340–362. https://doi.org/10.1111/FAF.12258

Smokorowski, K. E. (2022). The ups and downs of hydropeaking: a Canadian perspective on the need for, and ecological costs of, peaking hydropower production. *Hydrobiologia*, *849*, 421–441. https://doi.org/10.1007/s10750-020-04480-y

Takahashi, A., & Kurosawa, T. (2016). Regression correlation coefficient for a Poisson regression model. *Computational Statistics and Data Analysis*, *98*, 71–78. https://doi.org/10.1016/j.csda.2015.12.012

Tuhtan, J. A., Noack, M., & Wieprecht, S. (2012). Estimating stranding risk due to hydropeaking for juvenile European grayling considering river morphology. *KSCE Journal of Civil Engineering*, *16*(2), 197–206. https://doi.org/10.1007/S12205-012-0002-5

Watkinson, D. A., Ghamry, H. K., & Enders, E. C. (2020). *Canadian Science Advisory Secretariat (CSAS) Information to support the assessment of the Instream Flow Needs for Fish and Fish Habitat in the Saskatchewan River downstream of the E.B. Campbell Hydroelectric Station*. http://www.dfo-mpo.gc.ca/csas-sccs/

Wentworth, C. K. (1922). A Scale of Grade and Class Terms for Clastic Sediments. *The Journal of Geology*, *30*(5), 377–392. https://doi.org/10.1086/622910

Winemiller, K. O., McIntyre, P. B., Castello, L., Fluet-Chouinard, E., Giarrizzo, T., Nam, S., … Sáenz, L. (2016). Balancing hydropower and biodiversity in the Amazon, Congo, and Mekong. *Science*, *351*(6269), 128–129. https://doi.org/10.1126/SCIENCE.AAC7082/SUPPL_FILE/WINMEILLER-SM.PDF

Young, P. S., Cech, J. J., & Thompson, L. C. (2011). Hydropower-related pulsed-flow impacts on stream fishes: A brief review, conceptual model, knowledge gaps, and research needs. *Reviews in Fish Biology and Fisheries*, *21*(4), 713–731. https://doi.org/10.1007/S11160-011-9211-0/TABLES/2

Zarfl, C., Lumsdon, A. E., Berlekamp, J., Tydecks, L., & Tockner, K. (2015). A global boom in hydropower dam construction. *Aquatic Sciences*, *77*(1), 161–170. https://doi.org/10.1007/S00027-014-0377-0

SUPPORTING INFORMATION

Additional supporting information can be found online in the Supporting Information section at the end of this article.

How to cite this article: Glowa, S. E., Watkinson, D. A., Jardine, T. D., & Enders, E. C. (2023). Evaluating the risk of fish stranding due to hydropeaking in a large continental river. *River Research and Applications*, *39*(3), 444–459. https://doi.org/10.1002/rra.4083